1.E.1:
3.B

Nuclear Physics **83** (1966) 289—302; © *North-Holland Publishing Co., Amsterdam*

ENERGY LEVELS OF ^{106}Pd FED IN THE ^{106m}Rh DECAY

E. Y. DE AISENBERG and J. F. SUÁREZ

Comisión Nacional de Energía Atómica, Buenos Aires, Argentina

Received 14 January 1966

Abstract: The electron spectrum of ^{106m}Rh was analysed with an orange type magnetic spectrometer. Four components of the continuum spectrum were observed with end-point energies (in keV) and relative intensities: 1700±50 (0.7±0.2); 1310±20 (3.1±0.6); 920±10 (66±13) and 700±50 (30±13). The conversion electrons of 15 transitions have been observed. Their energies, with a relative error of about 1 %, and relative intensities are: 221 (525±75); 387 (125±50); 406 (275±125); 426 (300±140); 450 (160±60); 512 (1000); 616 (140±24); 717 (107±38); 1050 (50±10); 1124 (17±5); 1200 (19±6); 1255 (12±3); 1376 (5±2); 1530 (14±4) and 1566 (6±2). The energy of the 616 keV transition was more precisely determined with a double-focussing iron-yoke magnetic spectrometer as 616.0±0.4 keV.

Levels in ^{106}Pd are established at energies in keV of: 0, 511.8, 1127.8, 1228.9, 1557.4, 1931.8, 2039.6, 2076.4, 2084.1, 2305.6, 2350.3, 2365.5, 2756.4 and 2951.3 with spins and parities 0^+, 2^+, 2^+, 4^+, $(3, 4)^+$, $(4)^+$, 4^+, $(3\text{–}6)^+$, 3^+, $(3, 4, 5)^+$, $(4)^+$, $(3, 4, 5)^+$, 5^+, $(5, 6)^+$, respectively.

The total decay energy of ^{106m}Rh was determined to be 3675±10 keV. Spin and parity 6^+ is inferred for ^{106m}Rh.

Several features of the decay are explained by the asymmetric rotor theory of Mallmann.

E RADIOACTIVITY ^{106m}Rh [from ^{106}Pd(d, 2p); ^{108}Pd(d, α) and ^{109}Ag(n, α)]; measured $E_{\beta,\gamma}$, $I_{\beta,\gamma,ce}$, $\beta\gamma$-coin, cc, Q_β. ^{106}Pd deduced levels, J, π, log ft. Natural targets.

1. Introduction

It can be expected that some even nucleides of the $78 < A < 132$ region show rotational levels [1]). This is the case with ^{96}Mo and ^{110}Cd whose rotational levels can be predicted with an error (r.m.s.) of 4.4 and 4.7%, respectively [2]). As ^{106}Pd is farther from the closed shells, it may also have rotational spectra.

The level structure of ^{106}Pd has been studied experimentally [3]) through the beta decay of ^{106m}Ag (8.3 d) (refs. [4–7])), ^{106}Ag (24 min), ^{106}Rh (30 sec) and ^{106m}Rh (2.2 h) (refs. [8, 9])) and by Coulomb excitation methods [10]). As a consequence, the low-energy levels appear to be definitely established; however, in the higher energy region the energies, angular moments and parities are much more uncertain. In addition, the branching ratios of ^{106m}Rh beta decay have been previously determined only by scintillation techniques [9]) and the last scheme proposed [6]) does not show a satisfactory intensity balance.

2. Radioactive Sources

Sources of ^{106m}Rh were produced bombarding natural Pd with approximately 15 μAh of 28 MeV deuterons in the Buenos Aires synchrocyclotron. After irradiation

the Rh fraction was separated from the irradiated material by ion-exchange column methods [11]). Sources for use in the beta-ray spectrometers were then electroplated on a backing of $\approx$ 200 μg/cm^2 nickel foil. In addition to the ^{106m}Rh produced by the reactions ^{106}Pd(d, 2p)^{106m}Rh and ^{108}Pd(d, α)^{106m}Rh there was also present an appreciable quantity of other Rh activities which were readily identified by their half-lives.

A weaker source was also prepared by bombarding natural Ag with fast neutrons ($\approx$ 15 MeV) obtained from the Be(d, n) reaction. The separation of the rhodium activity from the target was made using a method similar to that adopted in the previous case. This source was not carrier-free and was used only to study the single gamma spectrum.

3. Instrumentation

The gamma spectrum was observed with a conventional 7.6 cm × 7.6 cm NaI(Tl) crystal spectrometer associated with a multi-channel analyser, placing the source at 40 cm from the crystal in order to make the sum peaks negligible. The Buenos Aires eight-gap orange type magnetic spectrometer at 2.0% momentum resolution was used to scan the electron spectrum and to measure beta-gamma coincidences. In this latter case the gamma detector was a 4.4 cm diam by 5.1 cm height NaI(Tl) crystal and a conventional fast-slow coincidence circuit (2τ = 50 nsec) was used to gate the multi-channel analyser.

The performance of the orange spectrometer for measuring continuous beta spectra was checked down to energies of 200 keV with ^{32}P sources on different backings and found to be quite satisfactory. By measuring the ^{90}Sr $\rightarrow$ ^{90}Y $\rightarrow$ ^{90}Zr beta decay, it was established that the intensities of the branches of a complex spectrum can be determined with an error of about 15%.

A double-focussing iron yoke magnetic spectrometer of the Svartholm-Siegbahn type at a 0.24% momentum resolution was also used.

4. Measurements and Results

4.1. SINGLE GAMMA SPECTRUM

The gamma spectrum of a source prepared by the ^{108}Pd(d, α)^{106}Rh and ^{106}Pd(d, 2p)^{106}Rh reactions is shown in fig. 1. The measurements were performed during a period of three months in order to establish the contributions due to ^{100}Rh (21 h), ^{101m}Rh (4.5 d), ^{101}Rh (206 d) and ^{105}Rh (35 h).

As a control of our procedure the spectrum obtained for ^{106m}Rh decay was compared with that obtained subtracting two spectra taken 2 h apart at the beginning of the measurements; as both spectra coincided within the statistical errors a detailed analysis was made (fig. 2). A source obtained from the ^{109}Ag(n, α)^{106m}Rh reaction was also studied in order to improve the results above 2.0 MeV and below 0.35 MeV, where the intense peaks at 307 keV (^{101m}Rh decay) and at 310 keV (^{105}Rh decay)

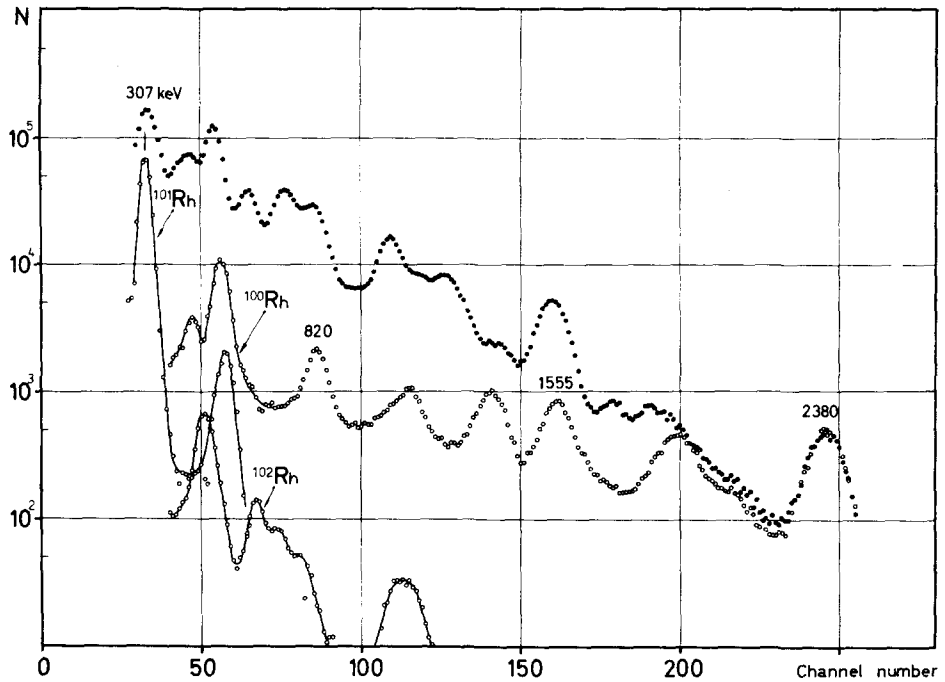

Fig. 1. The total direct γ-ray spectrum obtained with a 7.6 cm $\times$ 7.6 cm NaI(Tl) crystal showing the contributions of longer-lived Rh activities. The less significant contribution of ^{106}Rh below 320 keV is not shown.

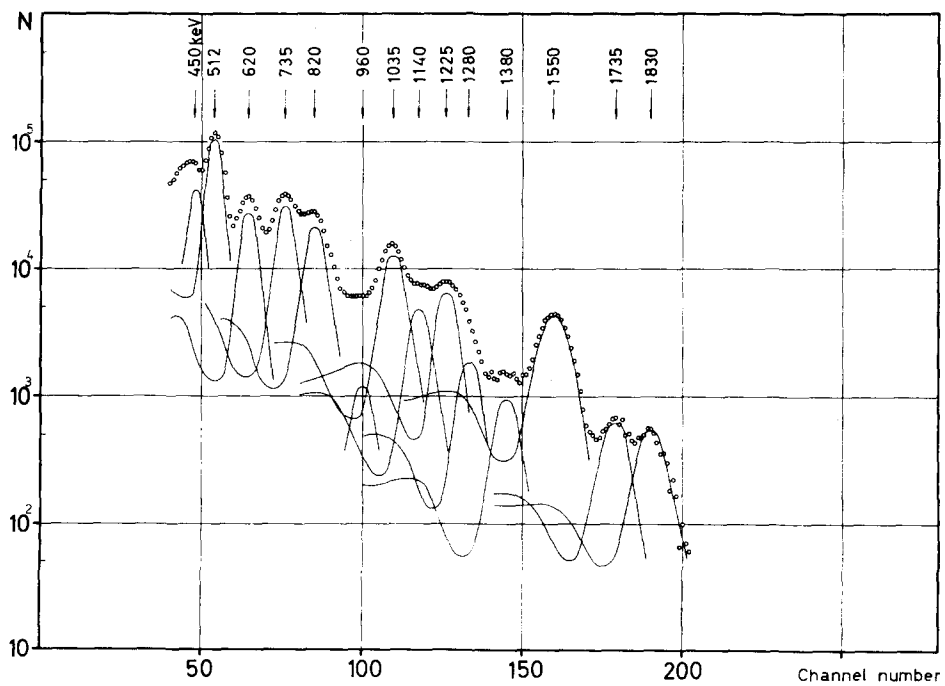

Fig. 2. Analysis of the ^{106m}Rh single γ-ray spectrum obtained from fig. 1. No correction due to bremsstrahlung was made.

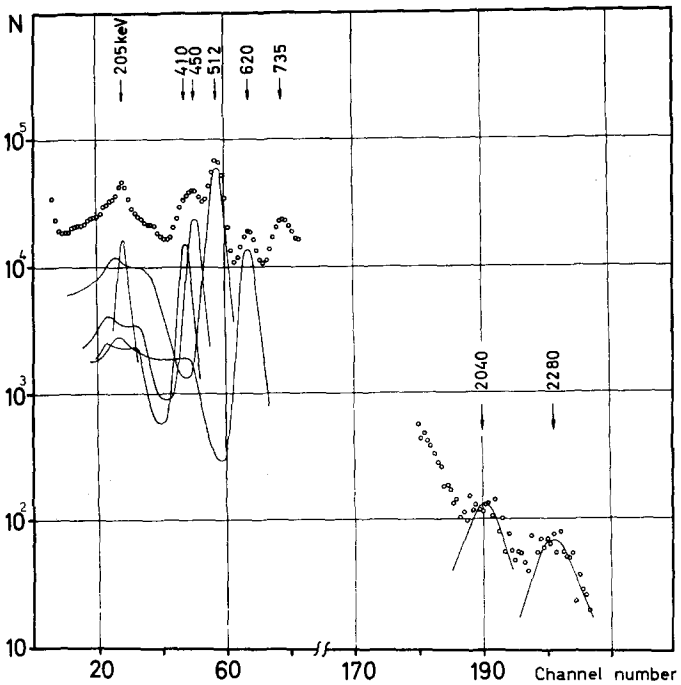

Fig. 3. Partial analysis of the ^{106m}Rh single γ-ray spectrum of a source obtained by the Ag(n, α)^{106m}Rh reaction. The source was at a distance of 5 cm from the 7.6 cm × 7.6 cm NaI(Tl) crystal.

TABLE 1

Relative intensities of γ-rays from ^{106m}Rh decay

	Present work			Ref. [8])	Ref. [9])
Energy (keV)	Pd(d, α)Rh	Ag(n, α)Rh	Adopted value		
205	9.8	7.3	8 ±2	18	20 ±4
410	24.6	19.0	22 ±4	43	20 ±4
450	37.4	34.8	36 ±8		35 ±5
512	100	100	100 ±10	100	100
620	36.0	33.0	34 ±5	26	33 ±5
735	52.2	56.3	54 ±6	36	47 ±8
820	42.6	45.8	44 ±6	45	40 ±6
960	3.0	5.3	4 ±1	?	3.5±1
1035	35.6	39.3	37 ±6	40	29 ±4
1140	15.4	12.8	14 ±5		14 ±2
1225	21.8	21.8	22 ±3	23	19 ±3
1280	6.8	5.0	6 ±1		
1380	3.8	6.2	5 ±1	?	
1550	21.4	26.0	24 ±3	23	21 ±3
1735	3.4	4.8	3.5±1	7	2 ±0.4
1830	3.3	5.4	3.5±1	8	2 ±0.4
2040	0.5	1.4	1.4±0.7	1	1 ±0.2
2280	0.5	0.9	0.9±0.4	1	0.5±0.1

have been subtracted introducing significant statistical errors. This source was measured during about 10 h at 5 cm from the crystal and the ^{105}Rh decay contribution deduced (fig. 3). The results are shown in table 1.

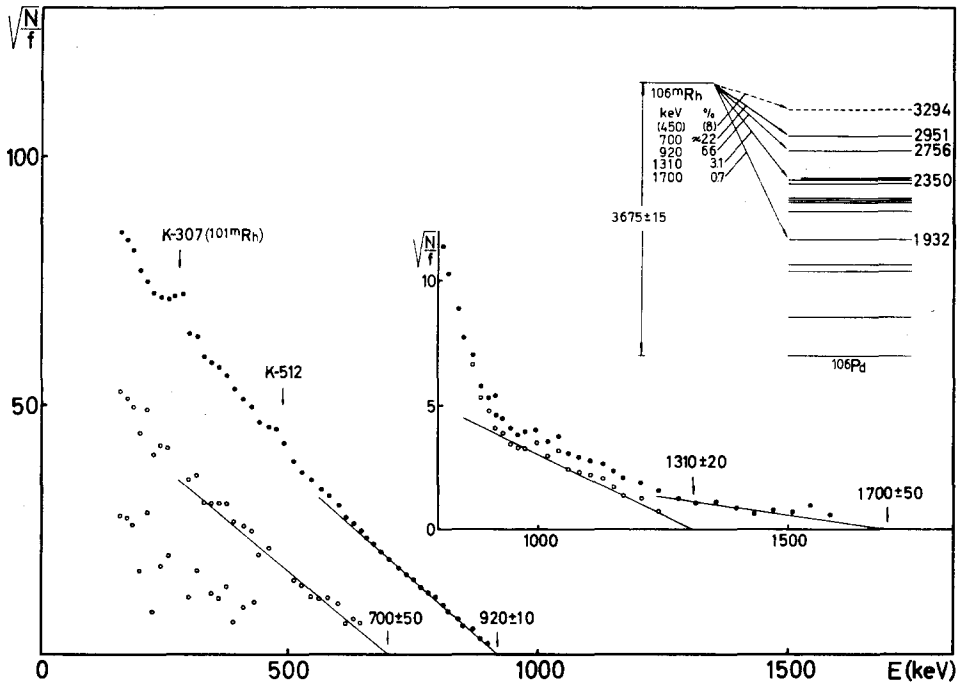

Fig. 4. Fermi plot of the beta spectrum of the 2.2 h activity. The relative intensities of the beta branches and log ft values are given in the inset.

TABLE 2

Partial β-ray spectra from ^{106m}Rh decay

Present work			Ref. [9])		
End-point (keV)	Intensity (%)	log ft	End-point (keV)	Intensity (%)	log ft
(450±100)	(8)				
700±50	22 ±13	5.5±1.0	790±40	40±4	5.3
920±10	66 ±13	5.3±0.2	950±30	38±4	5.6
1310±20	3.1±0.6	7.2±0.3	1180±30	11±2	6.5
1700±50	0.7±0.2	8.4±0.3	1620±20	10±2	7.1
>1700?	< 0.1				

4.2. THE CONTINUOUS BETA SPECTRUM

In fig. 4 the Fermi plot of the β-continuum and its components are shown. The inset shows the ^{106}Pd levels fed, as well as the Q-value proposed for ^{106m}Rh.

TABLE 3

Transition energies and gamma and K-line intensities in ^{106}Pd

Transition energies and relative K-line int				Gamma relative intensities from		
Previous investigations		Present work		Single gamma spectrum	Gamma-gamma coincidences [e]	I_{ce} and theoretical conv coef [f]
E (keV)	K-line intensity	E (keV)	K-line intensity			
110 1 [a, b]	21					
166 8 [a, b]	w					
194 93±0 15 [c]	44±6				1	0 3 ±0 1
221 51±0 10 [c]	630±50	221	525±75	8±2	7 ±3	5 65±1 67
228 53±0 12 [c]	67±8					0 72±0 17
282 0 [a]	w					
328 27±0 25 [c]	32±16				1 1±0 6	0 89±0 47
374 4 [a]	w					
390 90±0 20 [c]	98±25	387	125±50			4 8 ±1 3
396 5 [a, b]	w					
406 00±0 15 [c]	300±20	406	275±125	58±9	14 ±3	16 2 ±1 8
418 5 [a]	w					
429 46±0 15 [c]	260±20	426	300±140		14 ±5	16 8 ±1 6
450 80±0 20 [c]	160±15	450	160±60		23 ±5	11 7 ±1 3
457 3 [a, b]	w					
474 2 ±0 3 [b, c]	17±5	(479)	30±30			
511 77±0 20 [c]	1000±40	512	1000	100±10	100 ±10	100
585 7 [a]	w					

600 88±0 25 [c])	15±4					1 2 ±0 3
616 05±0 25 [c])	155±15	616.0	140±24	34±5	34	25 0 ±2 5
680 3 ±0 6 [c])	w					
703 3 ±0 5 [c])	30±10				4 5±1 0	6 6 ±2 2
716 2 ±0 4 [c])	130±10	717	107±38	54±6	17 ±2	11 ±2
717 1 ±0 4 [c])					20 ±8	21 ±2
737 6 [a, b])	w					
748 2 ±0 3 [c])	37±4				14 ±3	9 6 ±1 1
792 8 ±0 3 [c])	24±3				14 ±3	7 2 ±1 0
803 9 ±0 3 [c])	40±4				14 ±5	13 ±2
807 5 ±0 5 [c])	12±3			44±6	20±1 4	3 8 ±1 0
824 5 ±0 3 [c])	54±5				13 ±5	18 ±2
847 5 ±0 4 [c])	14±4				5 ±3	5 4 ±1 8
1045 7 ±0 4 [c])	48±4	1050	50±10	37±6	37 ±6	28 ±3
1127 8 ±0 5 [c])	13±3	1124	17±5	14±3	14 ±3	10 ±3
1199 1 ±0 6 [c])	13±4				14 ±3	11 ±4
		1200	19±6	22±3		
1222 8 ±0 6 [c])	8±3				6 ±3	6 ±3
		1255	12±3	6±1	6 ±1	10 ±3
1388 [d])	3 2	1376	5±2	5±1	5 ±1	5 ±2
1528 5 [a])	21	1530	14±4	24±3	16 ±2	18 ±5
		1566	6±2		6 ±3	8 ±3

[a]) Ref [6])
[b]) Neither these transitions nor the 2040 keV and 2280 keV transitions (table 1) are shown in the level scheme
[c]) Ref [7])
[d]) Ref [4])
[e]) Ref [5])
[f]) According to the case we have used the E2 or an average of E2 and M1 conversion coefficients

The results obtained in the present measurements are compared with those of Segaert *et al* [9]) in table 2 No shape could be assigned from the experiment

The measured continuous spectrum of ^{105}Rh, to be subtracted from the total continuum, was resolved into two components of end-point energies 570 and 250

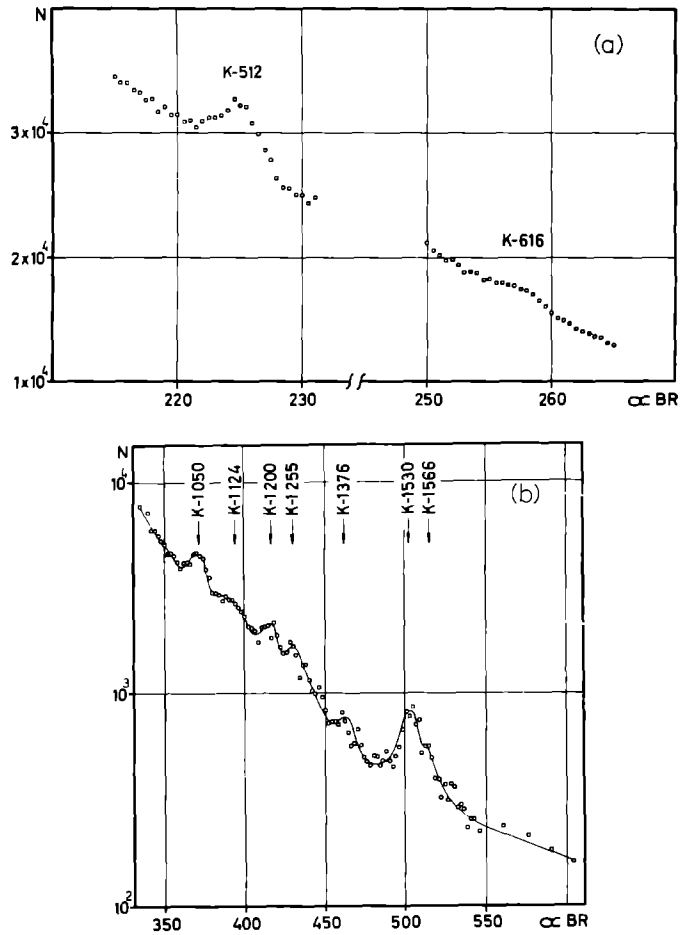

Fig 5 Conversion electron lines taken with a resolution of 2% in momentum The assignment for each line is indicated

keV with relative intensities 75±12 and 25±12, respectively, in agreement with previous experiments [12]).

4 3 THE CONVERSION ELECTRON SPECTRUM

A total of 15 conversion electron lines (see table 3 and fig 5) were observed and their energies and relative intensities determined The errors in the energy values are estimated to be about 1% except for the 616 keV transition, which was measured

with a double-focussing iron-yoke spectrometer. The value of 616.0 ± 0.4 keV obtained confirms that the transition originates at the second 2^+ level.

Below 900 keV the conversion electron lines are superimposed on the intense beta component of the continuous spectrum, and only those peaks whose intensity is larger than 10% of the 512 keV conversion peak intensity could be observed.

The conversion coefficient of the 512 keV transition was determined by comparing the area of its conversion line with the total area of the continuous beta spectrum and

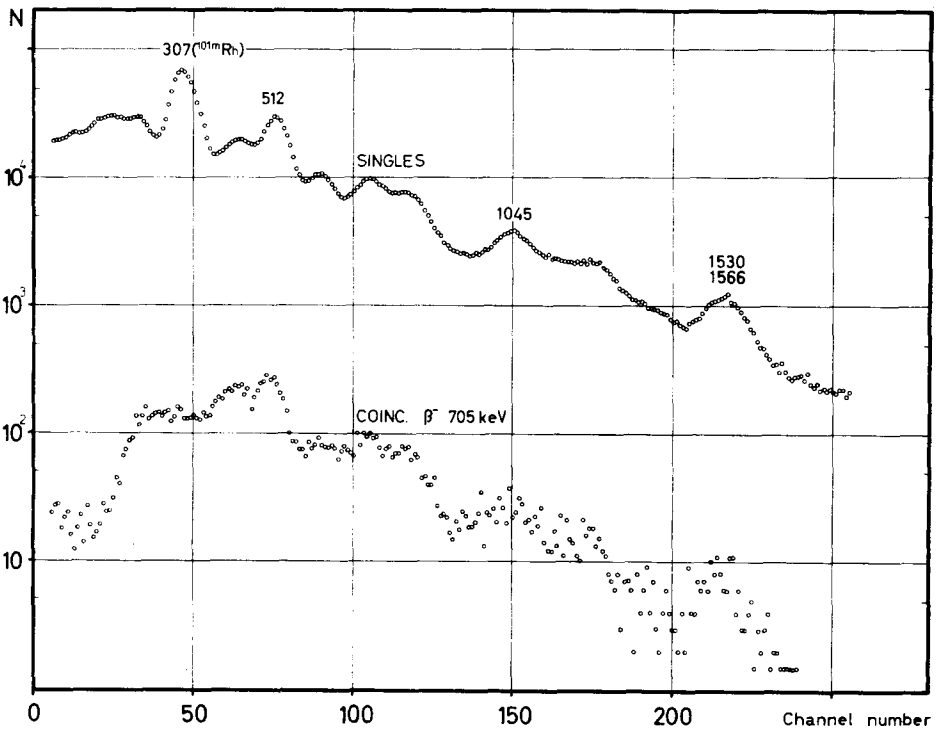

Fig. 6. Typical $\beta\gamma$-coincidence spectrum. Chance coincidences have been deduced.

taking into account the intensity of the 1124 keV ground state transition. The obtained value $[(4.9 \pm 1.1) \times 10^{-3}]$ is in agreement with the E2 character of this transition.

4.4. BETA-GAMMA COINCIDENCES

In order to determine the level fed by the intense beta component ($E = 920 \pm 10$ keV), two beta-gamma coincidence spectra were obtained with electron energies of 705 and 1120 keV, respectively. The first one, (fig. 6), when compared with the single gamma spectrum, showed a significant increase of the relative intensity of the 410–450 keV region. In the second one, the relative intensity of the 410–450 keV

region is still higher than in the single spectrum but the difference is less significant and the relative intensity of the region of 1200–1225 keV is clearly reduced. Due to the poor statistics no more information was obtained from this experiment, but it was possible to establish that the 920 keV beta branch feeds the 2756.4 keV level.

5. Discussion

The comparison of the present measurements with the gamma-ray energies and intensities reported by Robinson *et al.* [5]) and with the conversion electron energies and relative intensities reported by Scheuer *et al.* [7]) and Smith [6]), all in the decay of ^{106m}Ag, shows that most of ^{106}Pd levels are fed in a very similar manner in both de-

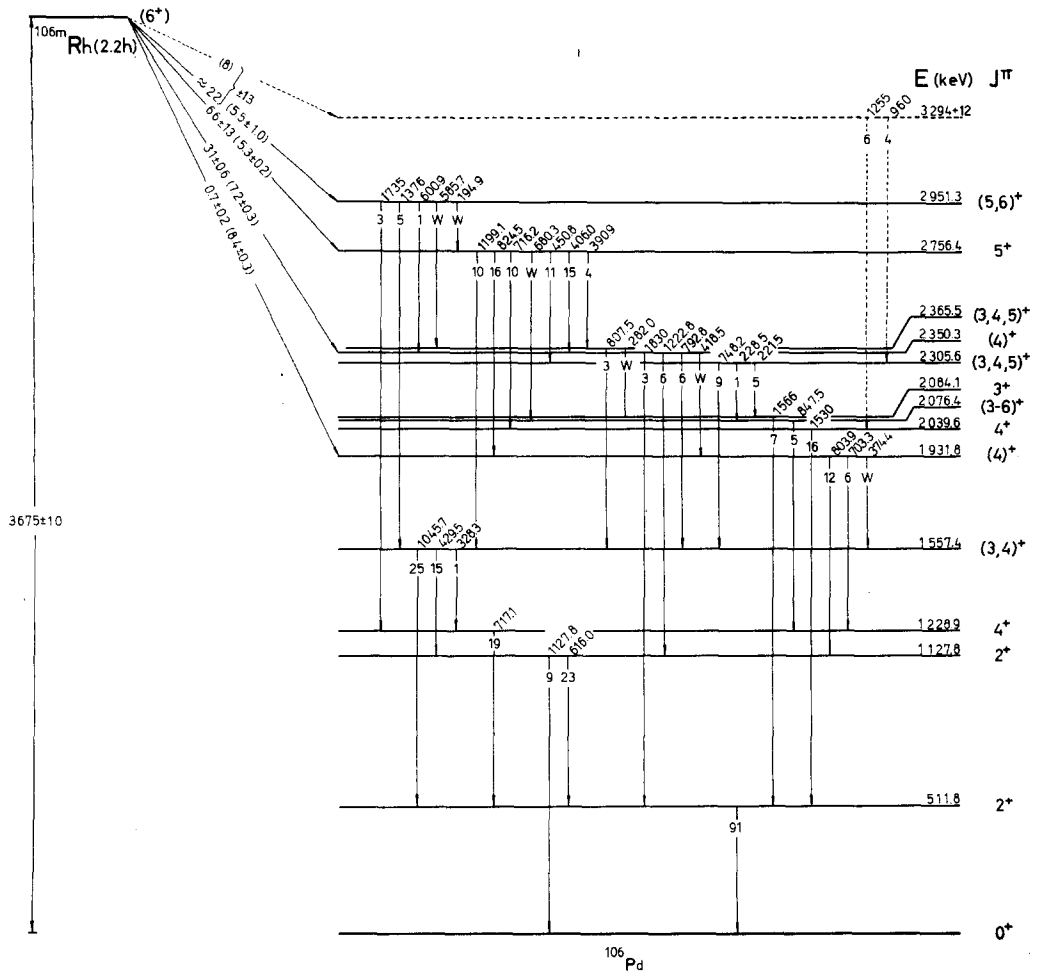

Fig. 7. Disintegration scheme of ^{106m}Rh (2.2 h). The intensities of the transitions are shown. The β-branches are those measured in this work.

cays. Thus the spin value $J = 6$ is preferred for ^{106m}Rh. The proposed level structure of ^{106}Pd is shown in fig. 7. This scheme is based on transition energies, energy-sum relations, gamma-gamma coincidences, beta-ray feedings, transition intensities and angular correlation data from both the ^{106m}Ag and ^{106m}Rh decays.

Regarding the transition energies, we have used the best available values [6,7]) up to 1222 keV and the present measurements for higher energies. As gamma-gamma coincidences in the ^{106m}Rm decay are much more difficult to measure than in the ^{106m}Ag decay, we have leaned heavily on the tables and graphs given by Robinson *et al.* The β-branchings shown are those obtained in the present work.

The experimental conversion coefficients were calculated with the values of columns 2 and 6 of table 3, normalizing to the theoretical E2 conversion coefficient of the 511.8 keV transition. Most of the transitions are E2 or E2+M1. Based on the proposed level scheme we assumed that all transitions are E2 or E2+M1 and using theoretical conversion coefficients and K-lines intensities, we calculated the gamma intensities shown in the last column of table 3. The transition intensities are obtained straightforwardly and used in fig. 7.

The characters assigned to the levels are based on the multipolarities obtained for the transitions, angular correlation data [5]), Coulomb excitation results for the low-energy levels [10]) and the log ft values determined in the present work.

The intensity balance is quite satisfactory, except for the 2076.4 keV level.

As a result, all but eight of the 44 reported transitions are included in the level scheme. Only two transitions have been observed in ^{106m}Rh decay and not in ^{106m}Ag decay: 960 ± 40 and 1255 ± 12 keV. We propose a level at 3294 ± 12 keV from which these two transitions arise. This level cannot be fed from ^{106m}Ag, whose Q-value [13,14]) is $\approx$ 3.1 MeV. The intensity obtained for the lowest energy beta branch should be interpreted as the branchings to the 2951.3 and 3294 keV levels.

Only two components of the continuous beta spectrum can be used to determine unambiguously the Q-value of ^{106}Rh, the 1700 ± 50 keV (0.7%) component which feeds the 1931.8 keV level and the 920 ± 10 keV (66%) component which feeds the 2756.4 keV level. The obtained Q-value is 3675 ± 10 keV.

Assuming the same log ft values for the negaton capture decay of ^{106m}Ag, its estimated Q-value gives 3100 ± 50 keV, in good agreement with the value measured in the Pd(p, n) reaction.

The proposed level scheme in general confirms that presented by Smith [6]), although a better intensity balance is obtained and more transitions are included.

Two of the levels proposed by Smith were removed, the 1702.7 keV level, due to a re-interpretation of gamma-gamma coincidences results [5]) and the weakly sustained 2738.4 keV level. The new proposed level at 2365.5 keV explains the 807.5 keV and three additional transitions. The 1530 keV transition de-excites the 2039.6 keV level formerly proposed by Robinson *et al.* at 2052 keV.

6. Theoretical Predictions

The predictions made with the quasi-adiabatic general asymmetric rotor model [1]) are, in this case, in better agreement with the experimental values than those obtained with the hydrodynamical model [15]). Assuming that the levels at 1127.8 and 1557.4

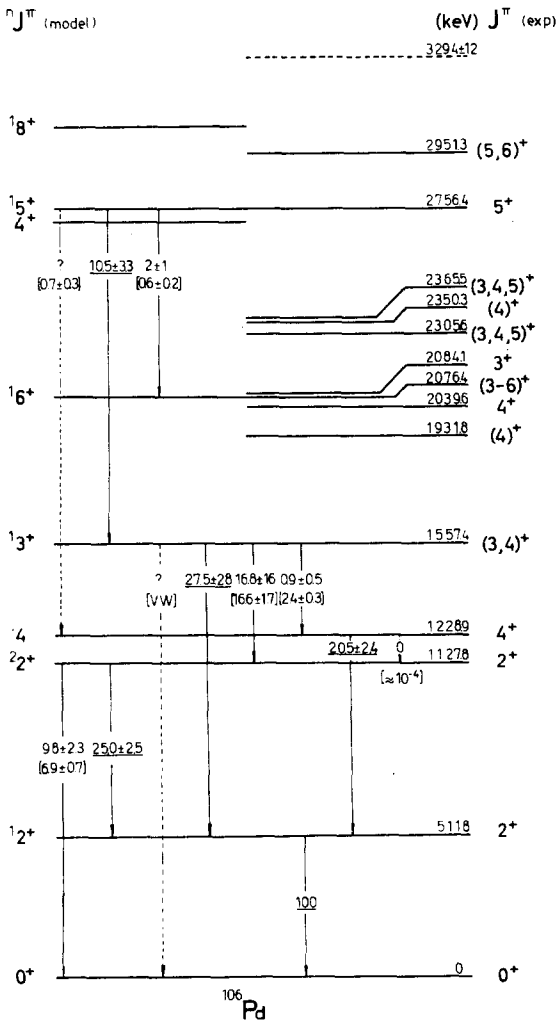

Fig. 8. Energy levels and transition probabilities predicted using the general asymmetric rotor model of the nuclei. The intensities computed are indicated in brackets.

keV are the $^{2}2$ and $^{1}3$, respectively, the $^{1}5$ level is predicted at 2640 keV and readily identified with the 2756.4 keV experimental level. Using the energy of the $^{1}4$ level the energies of the other levels are predicted. The $^{2}4$ and $^{1}8$ levels have not been experimentally observed. The $^{1}6$ level lies in a zone where three different energy levels are

proposed; we identified the 2076.4 keV level as the $^{1}6$ predicted by the model and obtained, finally, the following parameters for the rotor: $R_0(^{2}2) = 2.2890$; $k = 0.638$; $A/C = 6.594$ and $b = 0.001747$. The energies of the $^{1}2$, $^{2}2$, $^{1}4$, $^{1}3$, $^{1}5$ and $^{1}6$ levels are predicted with the following percent errors respectively 0, 0, 0, 1.0, −1.0 and 0.0. In fig. 8 the rotor levels and the experimental transitions and relative intensities are displayed. The experimental (2212)/(2210), (1314)/(1312), (1312)/(1322) and (1516)/(1513) intensity ratios were used to obtain the parameter $r = 0.650$ of the rotor, which was used to calculate the relative intensities of the transitions shown; these values, in brackets in the figure, are in good agreement with the experiment.

TABLE 4

The reduced transition probability ratios $b(\mathrm{E2}; n_J n'J')/b(\mathrm{E2}; n_J n''J'')$

	$\frac{b(2212)}{b(2210)}$	$\frac{b(1314)}{b(1322)}$	$\frac{b(1312)}{b(1322)}$	$\frac{b(1516)}{b(1513)}$	Parameters of the rotor	
Exp	52 ±2	11 ±6	0.019±0.003	3.3 ±2.0	k	r
BM	1.4	0.40	0	0	−1	0
DC	8.3	5.2	0.066	0.63	−0.47	0.40
M	74	29	0.019	0.76	0.64	0.65

Experimental results (Exp) are compared with predictions of different rotational models; Bohr and Mottelson (BM), Davydov and Chaban (DC) and Mallmann (M).

Table 4 shows the reduced transition probability ratios obtained using different rotational models, the k and r parameters in each case and the experimental results. The intrinsic quadrupole moment k_2 was calculated with Mallmann's model using the half-lives of the first [16]) and second excited states [3]); $k_2 = (3.1 \pm 0.1) \times 10^{-25}$ cm^2 and $k_2 = (2.7 \pm 1.3) \times 10^{-25}$ cm^2, respectively.

The authors wish to thank Lic. M. Induni de Rojas for the careful preparations of the sources and the synchrocyclotron technical staff for the numerous irradiations made. It is a pleasure to acknowledge discussions with the members of the beta-spectroscopy group.

This work was partially sponsored by the Consejo Nacional de Investigaciones Científicas y Técnicas, Argentina.

References

1) C. A. Mallmann, Nuclear Physics **24** (1961) 535
2) J. F. Suárez and E. Y. de Aisenberg, to be published
3) Nuclear Data Sheets
4) D. E. Alburger and B. J. Toppel, Phys. Rev. **100** (1965) 1357

5) R. L. Robinson, F. K. McGowan and W. G. Smith, Phys. Rev. **119** (1960) 1692
6) W. G. Smith, Phys. Rev. **131** (1963) 351
7) W. Scheuer, T. Suter, P. Reyes de Suter and E. Aasa, Nuclear Physics **54** (1964) 221
8) S. Mayo and S. J. Nassiff, Phys. Rev. **111** (1958) 1140
9) O. J. Segaert and L. J. Demuynck, Nuclear Physics **16** (1960) 492
10) D. Eccleshall, B. M. Hinds, M. J. L. Yates and N. MacDonald, Nuclear Physics **37** (1962) 377
11) M. Induni de Rojas, Radiochim. Acta **3** (1964) 167
12) S. E. Karlsson, O. Bergman and W. Scheuer, Ark. Fys. **27** (1964) 167
13) T. Enns, Phys. Rev. **56** (1939) 872
14) C. H. Johnson and A. Galonsky, Bull. Am. Phys. Soc. **5** (1960) 443
15) A. S. Davydov and A. A. Chaban, Nuclear Physics **20** (1960) 499
16) P. H. Stelson and F. K. McGowan, Phys. Rev. **110** (1958) 489